

OPTICAL STUDIES OF ARTIFICIAL OPALS AS 3D PHOTONIC CRYSTALS

D. Comoretto¹, D. Cavallo¹, G. Dellepiane¹, R. Grassi², F. Marabelli², L.C. Andreani², C.J. Brabec^{3,#}, A. Andreev³ and A.A. Zakhidov^{4,*}

¹ INFN - Dipartimento di Chimica e Chimica Industriale, Università di Genova, Italy.

² INFN - Dipartimento di Fisica "A. Volta", Università di Pavia, Italy.

³ Christian Doppler Laboratory for Plastic Solar Cells, J. Kepler University Linz, Austria.

⁴ Honeywell International Inc., Research and Technology, Morristown, USA.

#Present address SIEMENS AG, CTMM1- Innovative Electronics, D 91052 Erlangen, Germany.

*Present address Department of Physics, University of Texas Dallas, Dallas, USA.

ABSTRACT

Artificial opal films have been prepared by sedimentation of monodisperse silica spheres in water suspension. Atomic force microscope images show a triangular packing of the spheres at the surface of the films. The presence and the energy position of an optical pseudo gap in incidence-angle-dependent transmittance and reflectance spectra is observed and accounted for by theoretical calculations of the photonic band structure. These calculations indicate that the pseudo gap is due to the splitting of the photonic bands in the L point of the Brillouin zone. The spectroscopic data show additional loss structures due to both other features of the Brillouin zone and the diffraction of the light from the regular surface of the sample. The effect of the infiltration of opals with polydiacetylene solutions is also reported.

INTRODUCTION

Photonic band gap crystals are widely studied for their optical properties that allow manipulation of the flux of the light thus making these materials good candidates for all optical signal processing [1]. When the photonic crystal exhibits the suitable structure, all the characteristics depend on the dielectric contrast between the component media, one of them being typically the void. The possibility to fill the void with photosensitive materials like conjugated polymers or molecules, is promising for photo-switching devices [2].

Photonic crystals for different applications can be grown with periodicity of the dielectric constant in one, two or three dimensions. 1D or 2D photonic structures in a wide spectral range can be grown both with the top-down or the bottom-up approaches. At present, the growth of 3D photonic crystals with photonic band gap in the visible or ultraviolet spectrum by the techniques typical of the top-down approach like electron beam or X-ray lithography is a technological challenge. The alternative bottom-up approach, based on the self-assembly processes of suitable building blocks, is also widely used. Nanospheres of silica or polystyrene can be assembled into ordered 3D structures. Energetic considerations show that the face centered cube (fcc) packing with the (111) direction perpendicular to the film surface is the most favorite one [3]. In this way, artificial opals, which mimic the charm of the well-known gem-stones and show interesting photonic properties can be produced [4].

In this paper, we report on a morphological and optical study of silica artificial opal films by

using Atomic Force Microscopy (AFM) and variable incident angle polarized transmittance and reflectance spectroscopy. The results are accounted for on the basis of plane-waves calculations of the photonic properties of the opals. Preliminary results on the optical properties of these opals infiltrated with polydiacetylene solutions are also reported.

EXPERIMENTAL

Silica nanospheres with diameter $d=200$ and $d=370$ nm are obtained as previously reported [5]. The opal films are grown on glass, indium tin oxide covered glass or fused silica substrates by slow gravity sedimentation of the spheres in water suspension during several weeks. The films are used as grown without any annealing. Poly[1,6-bis(3,6-dihexadecyl-9H-carbazolyl-9-yl)hexa-2,4-diyne] (poly(DCHD-HS)) was prepared according to [6]. Atomic force microscopy (AFM) was performed by a Digital Instrument model NanoScope 3100 microscope in tapping mode. Variable incidence angle (θ , measured from the normal to the surface) polarized transmittance (T) and reflectance (R) measurements are performed with a double grating Varian spectrometer mod. Cary 5E. The light was linearly polarized by a Glan-Taylor prism. The cell used for the study of the photonic crystal infiltrated with poly(DCHD-HS) solutions is built with fused silica windows, one of them being the substrate of the opal film, separated by a fluorinated ethylene/propylene copolymer spacer 100 μm thick (Goodfellow).

RESULTS AND DISCUSSION

The AFM images of the films show that the surface is composed of regions where the spheres are both randomly disposed and orderly packed. The dimensions of these different domains is comparable ranging from about 10 to 50 μm . The largest ordered domains are obtained with the smaller spheres. Additional forms of disorder like sphere aggregates, dislocations and sphere vacancies can be observed. The propagation of these defects in the bulk of the film, which could give rise to stacking faults, cannot be at present excluded. In the ordered domains we observe a packing of the spheres in a triangular lattice, independently on d , as shown in Figure 1. A closer packing is observed for the smaller spheres.

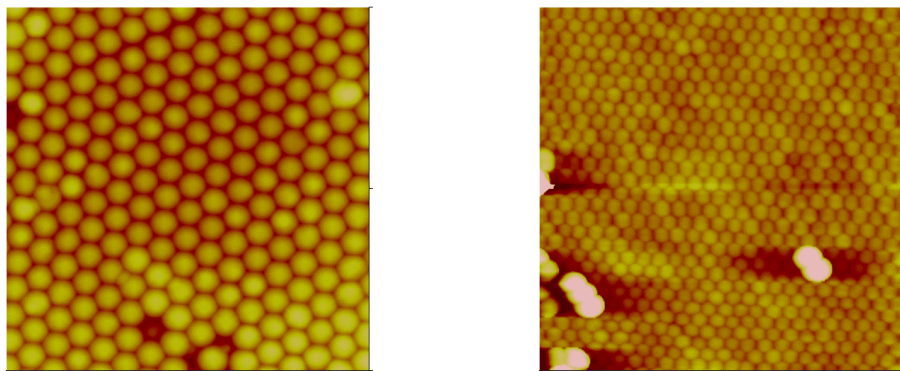


Figure 1. 5 μm x 5 μm AFM surface images of the silica opal films. Left panel $d=370$ nm, right panel, $d=200$ nm.

To obtain a 3D photonic crystal we need an ordered structure not only in the surface but also in the bulk. In our silica opal films we do not have any direct evidence of this ordering, which

has been instead observed for polystyrene opals, showing analogue surface properties. For the latter case indeed, the study of the cleaved edge of the films clearly shows the presence of balls packing in the fcc lattice [7]. Moreover, evidences of such a packing has been previously reported for silica opals [8].

Figure 2 shows the s-polarized variable-incident-angle T measurements for the opal films. For the p-polarization, not shown here, similar results are obtained. In the left panel, where the data for 370 nm spheres are reported, overlapped to a scattering background, an "absorption" due to the pseudo stop band of the opal at about 820 nm (0°) is evident. This feature uniformly shifts toward shorter wavelengths and reduces its intensity with increasing the incident angle. In addition, a reduction of the transmitted signal in all the spectral range by increasing the incident angle is observed. This effect is accompanied by a shift of the T edge from 450 to 650 nm as indicated in the figure by an arrow. This spectral shift, similar to that observed in the diffraction pattern of the film under white light illumination and related to the diffraction from the opal surface, will be separately discussed [7].

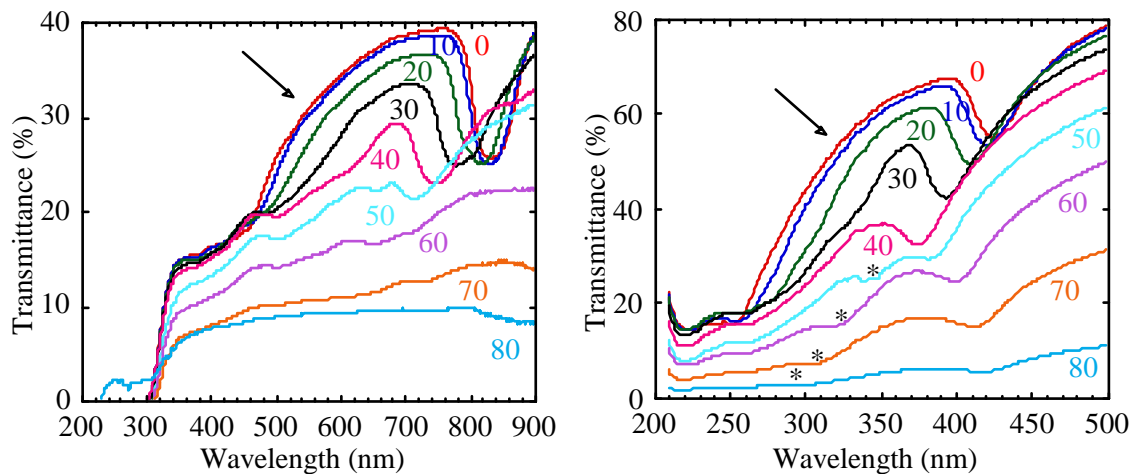


Figure 2. Variable incident angle T measurements in s-polarization of opal films. Left panel, $d=370$; right panel $d=200$ nm.

In the right panel, where the data for $d=200$ nm films are reported, the situation is more puzzling. The stop band, which at normal incidence is now peaked at about 430 nm due to the scaled ball size, exhibits a double behavior. Up to 40° , it shifts towards shorter wavelengths (as previously described) and for larger θ shifts back in the opposite direction. At the same time, a less pronounced set of features, marked by asterisks in the spectra, still shifts toward shorter wavelengths. By increasing θ , both the reduction of the T and its edge shift toward long wavelength (again highlighted with an arrow) are observed like in the case of $d=370$ nm.

In order to gain a better understanding of the optical properties of these opal films, we also performed polarized R measurements at different incident angles. These data, relative to s-polarization, are reported in Figure 3. For $d=370$ nm (left panel), a peak in the R spectra at almost the same wavelength observed in the corresponding T one is evident. The spectral position of this structure shifts toward shorter wavelength and its intensity roughly decreases by increasing the incidence angle. Below 500 nm, in particular for small incident angles, additional features, difficult to observe in the T spectra, are detected and attributed to the presence of domains with different orientation of the fcc sphere lattice in agreement with previous results for polystyrene opals [9]. At the end of these measurements, the film showed pronounced decreases

of its optical quality due to its poor mechanical properties which make opals very brittle. In fact, further measurements revealed a smearing out of the main R peaks as well as their broadening.

For the $d=200$ nm sphere sample, the main peak linearly shifts to shorter wavelength when the incident angle is increased. This behavior is strikingly different from that observed in the correspondent T spectra.

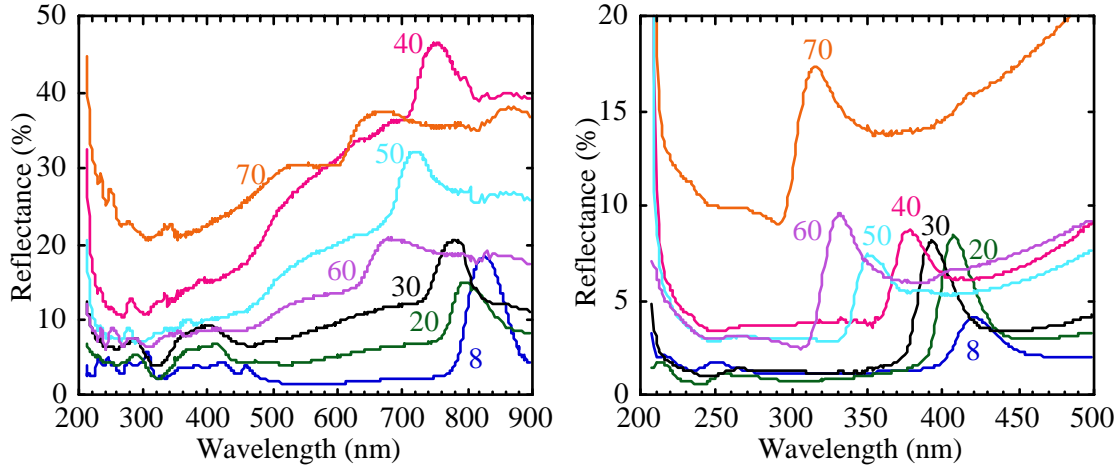


Figure 3. Variable incident angle reflectance measurements in s-polarization of opal film. Left panel $d=370$ nm; right panel, $d=200$ nm.

A rough analysis of the incident angle dependence of the spectra can be performed, in a first approximation, by considering the opal as a one-dimensional photonic crystal. In this case, the Bragg-Snell law provides a simple and useful relation between the wavelength of the stop band, the interplanar spacing in the (111) direction (D), the effective refractive index of the medium (n_{eff}) and θ [10]

$$\lambda = 2D\sqrt{n_{\text{eff}}^2 - \sin^2(\vartheta)} \quad (1)$$

D , in the case of close packing of the spheres, is strictly related to d ($D=d(2/3)^{0.5}$), and then the fit with (1) provides both the sphere radius which can be compared with the nominal value and the effective refractive index.

The results of this fit are shown in figure 4 and summarized in Table 1. The fit of the R data for 370 nm spheres is not reported here due to the poor reproducibility of these spectra. On the contrary, for the same sample the fitting of T provides a reasonable value of D , when compared with the value deduced assuming close packing of the spheres, as well as a good value of n_{eff} when compared with literature data [10]. More complicated is the analysis of the data for $d=200$ nm. The assumption of a strict relation among the data for $\theta=0^\circ$ to 30° with the small features at high energy for higher incident angles (* in Fig. 2), is confirmed by the fit where identical (\bullet, \blacklozenge) effective refractive index ($n_{\text{eff}}=1.31$) and inter-planar distance ($D=160$ nm) are obtained. This last datum is important because it is very close to that obtained for a close packed fcc $d=200$ nm sphere lattice (163 nm). For what the other features (\blacksquare) observed in T spectra are concerned, the fit provides a similar effective index but a very different value of D , probably related to a different set of crystallographic planes. A similar effect was observed for silica opals and attributed to the presence of both (111) and (220) planes [8]. A detailed analysis of the behavior

of this band on the basis of plane wave calculation of the photonic band structure and density of photonic states is in progress [7]. For the same sample, similar results are obtained from the R spectra. The value of n_{eff} is not unreasonable and D is also very close to that obtained from T spectra (\blacklozenge) thus allowing assignment of the corresponding features to the same origin. The fact that in the R spectra fewer features are observed than in the T one, is probably indicative of a higher defect density in the bulk with respect to the surface of the film. The pseudo stop band observed in the spectra, originating from planes separated by about 160 nm, can be assigned to the splitting of the photonic bands in the L point of the Brillouin zone on the basis of plane waves expansion calculations of the photonic structure of our opals.

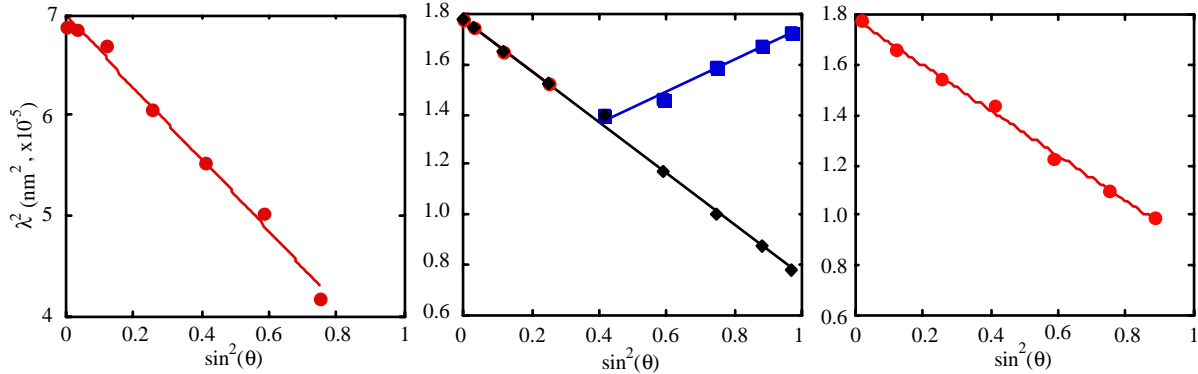


Figure 4. Equation (1) fit of the main features in the spectra of opal films. Left panel ($d=370$ nm), T. Middle panel ($d=200$ nm), T: circles, stop band for 0° , 10° , 20° and 30° ; diamonds, stop band and additional features (* in Fig. 2) for all investigated angles; squares, stop band for 40° , 50° , 60° , 70° and 80° . Right panel ($d=200$ nm), reflectance.

Table 1. D ($D=d(2/3)^{0.5}$) and n_{eff} relative to the data shown in Fig. 4 (same symbols).

T ($d=370$ nm)	T ($d=200$ nm)			R ($d=200$ nm)
\bullet	\bullet	\blacklozenge	\blacksquare	\bullet
$D=298$ nm (302 nm)	$D=161$ nm (163 nm)	$D=160$ nm (163 nm)	$D=124$ nm (163 nm)	$D=149$ nm (163 nm)
$n_{\text{eff}}=1.40$	$n_{\text{eff}}=1.31$	$n_{\text{eff}}=1.31$	$n_{\text{eff}}=1.35$	$n_{\text{eff}}=1.41$

We also would like to show here preliminary studies on the infiltration of the opal films with toluene solutions of poly(DCHD-HS), a conjugated polymer showing interesting non-linear optical properties [11]. Infiltration of opal with solutions is our first step toward a solid state infiltrated polyDCHD-HS (inverted opal) photonic crystal.

Figure 5 shows the variable incident angle transmission measurements of a $d=200$ nm opal film infiltrated with a solution of poly(DCHD-HS) in toluene. The spectrum of the solution, discussed in detail in ref. [6], is also reported for comparison. Even though these data are very preliminary some conclusion can be drawn. The refractive index of this diluted solution is very similar to that of the solvent ($n=1.497$) thus providing a rough index matching situation with the photonic crystal. This fact reduces the Rayleigh scattering background observed in the spectra of figure 2 and efficiently smoothes the photonic stop band as pointed out by the lack of its feature in the spectrum. Only for large incident angle a small structure, evidenced by the pointers, can be detected. The position of the stop band is overlapped to the high-energy part of the absorption

spectrum of poly(DCHD-HS) and very close to the transitions of the carbazolyl side group. Due to the index matching condition, no particular effect is here detected, but a proper choice of the sphere diameter can shift the stop band in the near infrared where an interesting photophysics related to triplet excitons has been detected [12].

Our future goal is that of producing such opals, infiltrating them with polydiacetylenes and then studying the photophysics of such materials inside the photonic crystal.

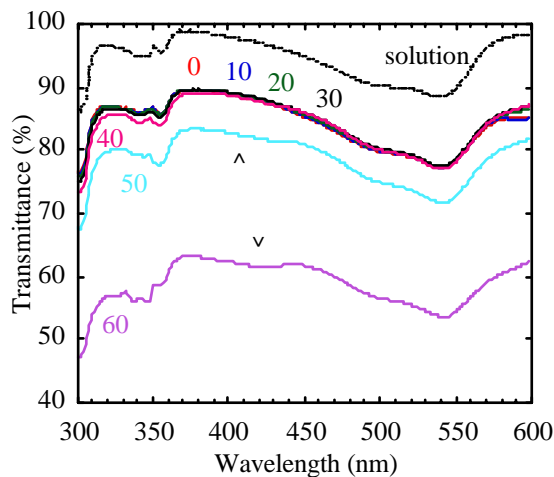


Figure 5. $d=200$ nm opal film filled with poly(DCHD-HS) toluene solution for different incident angles. The spectrum of the free solution is also reported for comparison (dashed line).

REFERENCES

1. J.D. Joannopoulos, R.D. Meade, J.N. Win, *Photonic Crystals*, Princeton University press, Singapore (1995).
2. Z.Z. Gu, T. Iyoda, A. Fujishima, and O. Sato, *Adv. Mater.* **13**, 1295 (2001).
3. S.-C. Mau and D.A. Huse, *Phys. Rev.* **E59**, 4396 (1999).
4. For a review on this argument see *Adv. Mater.* **13** (2001).
5. A.A. Zakhidov, R.H. Baughman, Z. Iqbal, C. Cui, I. Khayrullin, S.O. Dantas, J. Marti, and V.G. Ralchenko, *Science* **282**, 897 (1998).
6. M. Alloisio, A. Cravino, I. Moggio, D. Comoretto, S. Bernocco, C. Cuniberti, C. Dell'Erba, and G. Dellepiane, *J. Chem. Soc., Perkin Trans. 2*, 146 (2001).
7. D. Comoretto, in preparation.
8. H.Miguez, C. Lopez, F. Meseguer, A. Blanco, L. Vasquez, R. Mayoral, M. Ocaña, V. Fornés, and A. Mifsud, *Appl. Phys. Lett.* **71**, 1148 (1997). V. Colvin, *MRS Bulletin* **26**, 637. W.L. Vos and H.M. van Driel, *Phys. Lett.* **A272**, 101 (2000).
9. P. Nozar, C. Dionigi, M. Muccini, C. Taliani, *Adv. Mater.*, submitted.
10. W.L. Vos, R. Sprik, A. van Blaaderen, A. Imhof, A. Lagendijk, and G.H. Wegdam, *Phys. Rev.* **B53**, 16231 (1996).
11. S. Sottini, G. Margheri, E. Giorgetti, F. Gelli, A. Cravino, D. Comoretto, C. Cuniberti, C. Dell'Erba, I. Moggio, and G. Dellepiane, *Non Linear Optics* **25**, 385 (2000).
12. G. Lanzani, G. Cerullo, M. Zavelani-Rossi, S. De Silvestri, D. Comoretto, G. Musso, and G. Dellepiane, *Phys. Rev. Lett.* **87**, 7402 (2001).